Vanadium Azides

DOI: 10.1002/anie.200906537

The Syntheses and Structure of the Vanadium(IV) and Vanadium(V) Binary Azides $V(N_3)_4$, $[V(N_3)_6]^{2-}$, and $[V(N_3)_6]^{-}$[**]

Ralf Haiges,[*] Jerry A. Boatz, and Karl O. Christe[*]

In memory of Robert Bau

During the last decade, there has been much interest in inorganic polyazide chemistry.[1–16] Because of the energetic nature of the azido group, polyazides are highly endothermic compounds, the energy content of which increases with an increasing number of azido ligands. It is, therefore, not surprising that the synthesis of molecules with a high number of azido groups is very challenging owing to their explosive nature and shock sensitivity.

A significant number of pentavalent binary azido compounds of the heavier Group 5 elements have been prepared and characterized, namely $Nb(N_3)_5$, $Ta(N_3)_5$, $Nb(N_3)_5{\cdot}CH_3CN$, $Ta(N_3)_5{\cdot}CH_3CN$, $[Nb(N_3)_6]^-$, $[Ta(N_3)_6]^-$, $[Nb(N_3)_7]^{2-}$ and $[Ta(N_3)_7]^{2-}$.[14,15] However, the situation is different for vanadium for which only trivalent binary azides were known. Thus, the UV/Vis spectra of solutions containing the ions $[V(N_3)]^{2+}$, $[V(N_3)_4]^-$, and $[V(N_3)_6]^{3-}$,[17] and also the vibrational and electronic spectra of the $[V(N_3)_6]^{3-}$ ion[18] have been reported. For the higher oxidation states of vanadium, only ternary or quatenary azides, such as $VOCl_2N_3$,[19] $[VO(N_3)_4]^{2-}$,[18,20,21] and $[V(N_3)_3(N_3S_2)]^{2-}$,[22] have been reported, and no binary vanadium(V) compounds are known except for VF_5, VF_6^-, and V_2O_5.

By analogy with our previous syntheses of binary Group 5 azides,[14] vanadium fluorides were reacted with an excess of Me_3SiN_3 in acetonitrile solution. Contrary to the incomplete halide/azide ligand exchange frequently encountered for chlorides, the use of fluorides as a starting material results in rapid and quantitative fluoride/azide exchange. Thus, for VF_4, a dark red, almost black solution of $V(N_3)_4$ [Eq. (1)] was obtained in quantitative yield.

$$\mathrm{VF_4 + 4\,Me_3SiN_3 \xrightarrow{CH_3CN} V(N_3)_4 + 4\,Me_3SiF} \qquad (1)$$

As expected for a covalently bonded polyazide,[23] solid $V(N_3)_4$ is very shock-sensitive. It can explode violently upon the slightest provocation, for example when touched with a metal spatula or by a rapid change in temperature (such as freezing with liquid nitrogen or a fast warm-up). All attempts to obtain single crystals of $V(N_3)_4$ by recrystallization were unsuccessful. The identity of the vanadium tetraazide was established by the observed weight, a low-temperature Raman spectrum, and by quantitative conversion with either $Ph_4P^+N_3^-$ or $PNP^+N_3^-$ (PNP^+ = bis(triphenylphosphoranylidene)ammonium) into the corresponding $[V(N_3)_6]^{2-}$ salts. These salts were characterized by their material balances, crystal structures, and vibrational spectra of the crystals and the bulk material, which were identical. The recording of the Raman spectrum of $V(N_3)_4$ was very challenging owing to the black color of the sample, its amorphism, and its extreme shock sensitivity. In spite of these difficulties, we succeeded to record several reproducible Raman spectra of amorphous samples and one spectrum of a crystalline sample before it exploded. In the Supporting Information, Table S16, the vibrational frequencies and intensities observed for the amorphous samples are compared with those calculated for the free molecular species at the MP2/MCP-TZP level of theory. The vibrational frequencies calculated for $V(N_3)_4$ at the B3LYP/MCP-TZP level are given in the Supporting Information, Table S1. There is a very good agreement between the calculated and observed frequencies (Supporting Information, Table S16), suggesting that amorphous $V(N_3)_4$ is only weakly associated and permits assignments to the individual modes. In contrast, the Raman spectrum obtained for the crystalline sample (Supporting Information, Table S16, footnote [a]) deviated significantly from that of the amorphous sample. It showed three intense bands in the region of the V-N stretching modes, indicating association.

The MP2/MCP-TZP calculations resulted in a minimum energy structure of S_4 symmetry, with a V–N bond length of 1.841 Å. At this level, the D_{2d} isomer is not a local minimum, has four imaginary frequencies, and is 6.2 kcal mol^{-1} higher in energy than the S_4 isomer. At the B3LYP/MCP-TZP level, the D_{2d} structure, with a longer V–N bond length of 1.870 Å

---

[*] Dr. R. Haiges, Prof. Dr. K. O. Christe
Loker Research Institute and Department of Chemistry
University of Southern California
Los Angeles, CA 90089-1661 (USA)
Fax: (+1) 213-740-6679
E-mail: haiges@usc.edu
kchriste@usc.edu

Dr. J. A. Boatz
Space and Missile Propulsion Division
Air Force Research Laboratory (AFRL/RZSP)
10 East Saturn Boulevard, Edwards Air Force Base, CA 93524 (USA)

[**] This work was funded by the Air Force Office of Scientific Research, the Office of Naval Research, the Defense Threat Reduction Agency, and the National Science Foundation. We thank Profs. G. Olah and S. Prakash for their steady support, and Drs. W. Wilson and R. Wagner for their help and stimulating discussions. Grants of computer time from the Department of Defense High Performance Computing Modernization Program at the Engineer Research and Development (ERDC) and Navy Department of Defense Supercomputing Centers are gratefully acknowledged.

Supporting information for this article, including the Experimental Section, is available on the WWW under http://dx.doi.org/10.1002/anie.200906537.

(Supporting Information, Tables S2, S3, and S17), is slightly favored by 0.3 kcal mol^{-1} over the S_4 isomer. Both structures are similar and can be derived from tetrahedral VN_4 skeletons in which two of the bond angles are slightly compressed whilst the other four are widened. However, there is a difference in the arrangement of the floppy azido ligands. In the S_4 isomer, the two compressed angles are opposite to each other, whereas in the D_{2d} isomer they are neighboring. Generally, in S_n-type structures (the C_i structure of $V(N_3)_6{}^{2-}$; Supporting Information, Table S17) is also a slightly distorted S_6 structure), the azido ligands are arranged in a propeller-type fashion, whilst in D_{nd}-type structures the presence of an additional mirror plane along the n-fold inversion axes forces the azido ligands into arrangements that are symmetric to this plane. In view of the complexity of the spectra, their low sensitivity to minor rearrangements of the ligands, the expected fluxionality of the structures, and experimental difficulties in recording them with sufficient resolution at low temperatures in the solid state to freeze out ligand rotation, a clear distinction between these two geometries is very difficult. However, it appears that for these polyazides the propeller-type ligand arrangements of S_n symmetry are generally favored over the D_{nd} structures, and therefore the S_4 structure is also preferred by us for $V(N_3)_4$.

As found for other neutral binary polyazides,[8–15] $V(N_3)_4$ can also be stabilized by anion formation, which increases the ionicity of the azido group. Because an ionic azide group possesses two double bonds whereas a covalent azide group has a single and a triple bond, increasing the ionicity of an azido ligand makes the breaking of an N–N bond more difficult and enhances the activation energy barrier toward N_2 elimination. To verify these predictions, the hexaazidovanadate(+IV) anion $[V(N_3)_6]^{2-}$ was prepared as its tetraphenylphosphonium $[PPh_4]^+$ and bis(triphenylphosphoranylidene)ammonium salts $[PNP]^+$ by the reactions of $V(N_3)_4$ with two equivalents of AN_3 ($A = PPh_4$, PNP) in acetonitrile solution [Eq. (2)].

$$V(N_3)_4 + 2\,AN_3 \xrightarrow{CH_3CN} [A]_2[V(N_3)_6] \qquad A = PPh_4,\ PNP \tag{2}$$

$[PPh_4]_2[V(N_3)_6]$ and $[PNP]_2[V(N_3)_6]$ were isolated as room-temperature-stable, crystalline solids of dark maroon to nearly black color that melt with gas evolution and decomposition at 175–177 and 169–172 °C, respectively. Because of the increased ionicity of their azido ligands and the presence of two large counterions per anion, which diminishes shock propagation, both compounds are less sensitive and explosive than the parent compound, $V(N_3)_4$, and could be manipulated in our studies at room temperature without explosions. Scraping with a metal spatula or heating in an open flame did not result in detonations.

The $[PPh_4]_2[V(N_3)_6]$ and $[PNP]_2[V(N_3)_6]$ salts were characterized by the observed weights, their IR and Raman spectra (see the Supporting Information), and their crystal structures.[24] The Raman spectra of the crystals used for the X-ray investigation and of the bulk material were identical, demonstrating the absence of detectable amounts of impurities in our samples.

The theoretical calculations predict two possible structures of very similar energy, having C_i and D_{3d} symmetry, respectively (Supporting Information, Table S17). The C_i structure has a slightly distorted, propeller-type S_6 structure. At the B3LYP/MCP-TZP level, it is favored by 4.2 kcal mol^{-1} over a D_{3d} structure. However, at the MP2/MCP-TZP level of theory, a D_{3d} structure is slightly lower in energy by 0.9 kcal mol^{-1}. In view of their small energy differences and sensitivity to the level of theory used, the theoretical predictions do not allow the reliable prediction of a preferred structure, even for the free gaseous species at 0 K. For molecules of this size, the use of more definitive higher-level calculations, such as CCSD(T), is prohibitive from a computational point of view. Although the theoretical calculations predict for the C_i and D_{3d} structures of $[V(N_3)_6]^{2-}$ different numbers of fundamental vibrations for the antisymmetric N_3 stretching vibrations, namely, 6 for C_i and only 4 for D_{3d} (Supporting Information, Tables S4, S5), four of the C_i modes fall within a narrow range of only 7 cm^{-1} and would be extremely difficult to resolve. Furthermore, the small energy difference between the two isomers and the fluxionality of the azido ligands, combined with very shallow energy minima and minimal barriers, should result for the free ion in the experimental observation of a single band in this region. As several shoulders, weak bands, and violations of the selection rules were observed in the solid-state spectra of $[PPh_4]_2[V(N_3)_6]$ and $[PNP]_2[V(N_3)_6]$, the infrared spectra of the salts in CH_3CN solution were recorded in this region and showed, as expected, a collapse into a single band at 2040 cm^{-1} with a large linewidth of 35 cm^{-1}. Therefore, the splittings in the solid-state spectra are attributed to packing effects and the influence of different counterions. The solution spectra also allowed the decomposition of $[V(N_3)_6]^{2-}$ in CH_3CN solution to be observed when exposed to air. The 2040 cm^{-1} band would gradually decrease in intensity, while the dark purple vanadium(IV) color changed to the green color that is characteristic for vanadium(III). At the same time, an intense band at 2004 cm^{-1} grew in, which was subsequently replaced by bands at 2060(vs), 2093(mw), and 2138(m), with the band at 2138 cm^{-1} being attributed to HN_3. As the crystal structure analysis established C_i structures for both the $PPh_4{}^+$ and the PNP^+ salts,[24] assignments of the observed vibrational spectra to individual modes were made for this isomer by comparison with the calculated spectra and resulted in very good agreement (Supporting Information, Table S4; for the calculated vibrational spectra of the D_{3d} isomer, see the Supporting Information, Table S5).

The structures of $[PPh_4]_2[V(N_3)_6]$ and $[PNP]_2[V(N_3)_6]$ were established by single-crystal X-ray diffraction studies (Figure 1; Supporting Information, Figures S5, S6, Tables S6–S15). Although the refined structure of $[PPh_4]_2[V(N_3)_6]$ had a low R_1 factor of 6.66 %, it suffered from some disorder resulting in a high wR_2 factor of 17.57 % and variations in the individual bond lengths and angles that are much larger than those found for the PNP^+ salt. As the vibrational spectra of the anions were identical for all practical purposes in both salts, the increased distortion from S_6 symmetry of the anion in the $PPh_4{}^+$ salt is not real and is an artifact of the disorder. Consequently, only the structure of the PNP^+ salt will be

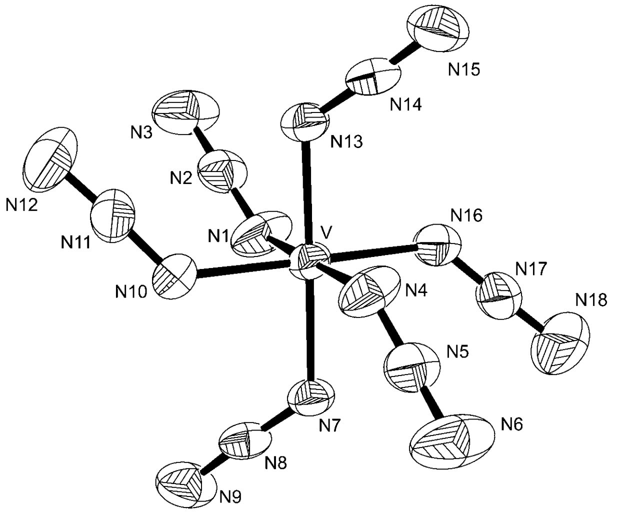

Figure 1. ORTEP drawing of the $[V(N_3)_6]^{2-}$ anion in $[PNP]_2[V(N_3)_6]$. Thermal ellipsoids are set at 50% probability. Selected bond lengths [Å] and angles [°]: V–N1 1.991(3), V–N4 1.992(3), V–N7 1.990(3), V–N10 2.002(3), V–N13 1.988(3), V–N16 2.001(3), N1–N2 1.178(4), N2–N3 1.153(4), N4–N5 1.181(4), N5–N6 1.136(4), N7–N8 1.211(4), N8–N9 1.148(4); V-N1-N2 128.1(3), V-N4-N5 127.5(3), V-N7-N8 125.6(2), V-N10-N11 128.3(2), V-N13-N14 123.5(3), V-N16-N17 130.3(2), N1-V-N4 177.50(13), N1-V-N7 90.69(12), N1-V-N10 90.77(14), N1-V-N13 91.25(12), N1-V-N16 87.991(15), N1-N2-N3 176.8(4), N4-N5-N6 177.0(4), N7-N8-N9 176.9(3).

discussed in more detail, as it does not suffer from any disorder. The X-ray crystal structure of the $[PNP]_2[V(N_3)_6]$ salt[24b] revealed the presence of well-separated $[PNP]^+$ and $[V(N_3)_6]^{2-}$ ions (Supporting Information, Figure S6). The closest V···N and N···N contacts between neighboring anions are 7.9 Å and 4.2 Å, respectively. The observed geometry of the $[V(N_3)_6]^{2-}$ anion (Figure 1) is in good general agreement with the propeller-type C_i structure predicted by our theoretical calculations (Supporting Information, Table S17) and those previously found for the similar hexaazides $[As(N_3)_6]^-$,[6,23] $[Sb(N_3)_6]^-$,[11] $[Si(N_3)_6]^{2-}$,[4] $[Ge(N_3)_6]^{2-}$,[3] $[Nb(N_3)_6]^-$,[14] $[Ta(N_3)_6]^-$,[14] $W(N_3)_6$,[13] $[Ti(N_3)_6]^{2-}$,[12] and $[Se(N_3)_6]^{2-}$,[25] but contrary to that of $[Te(N_3)_6]^{2-}$,[8] for which the free valence electron pair on its central atom becomes sterically active.

The VN_6 skeleton of the $[V(N_3)_6]^{2-}$ anion has almost perfect S_6 symmetry. Selected bond lengths and angles are listed in Figure 1 and the Supporting Information, Table S13. The observed average V–N distance of 1.994 Å is shorter than the calculated values (B3LYP 2.027 Å, MP2 2.005 Å) and the observed average V–N distances in $(\eta^5\text{-}C_5H_5)_2V(N_3)_2$ (2.080 Å),[26] $[V(N_3)_3(N_3S_2)]_2^{2-}$ (2.02 Å),[27] and the terminal azido group in $[(\eta^5\text{-}C_5Me_5)VCl(N_3)(\mu\text{-}N_3)]_2$ (2.058 Å),[28] and similar to the observed V–N distance for the terminal azido groups in $[(\eta^5\text{-}C_5Me_5)V(N_3)_2(\mu\text{-}N_3)]_2$ (1.981 Å).[28] The observed V–N distances of the $[V(N_3)_6]^{2-}$ anion are more than 0.12 Å longer than those calculated for the neutral parent compound $V(N_3)_4$ (Supporting Information, Table S17). This increase in bond length can be explained by the higher ionicity of the V–N bonds in $[V(N_3)_6]^{2-}$ caused by the two formal negative charges. The observed and calculated N–N bond lengths serve as further evidence for the increased ionicity of the azide ligands in $[V(N_3)_6]^{2-}$. The two N–N distances of the N_3 groups in $V(N_3)_4$ are calculated by B3LYP to differ by 0.098 Å (MP2 0.053 Å), indicating the presence of predominantly covalent azido groups with strong N_β–N_γ triple-bond character. In the $[V(N_3)_6]^{2-}$ anion, the differences in the N–N distances of the azido groups are predicted to be smaller (B3LYP C_i 0.049, D_{3d} 0.044 Å; MP2 C_i 0.023, D_{3d} 0.021 Å) and were experimentally found to range from 0.023 to 0.063 Å, with an average value of 0.043 Å. These smaller differences in the N–N bond distances support our conclusion that the azido ligands in the anion are more ionic in character.

Our attempts to prepare $V(N_3)_5$ were unsuccessful. Even at a temperature of −35 °C, the reaction of VF_5 with an excess of Me_3SiN_3 in acetonitrile solution resulted in the release of elemental nitrogen and the reduction of V^V to V^{IV}, yielding a dark red, almost black solution of $V(N_3)_4$ [Eq. (3)].

$$2\,VF_5 + 10\,Me_3SiN_3 \xrightarrow{CH_3CN} 2\,V(N_3)_4 + 10\,Me_3SiF + 3\,N_2 \qquad (3)$$

Pumping off the volatile compounds at ambient temperature resulted in the isolation of the neat tetraazide as an amorphous black solid.

The preparation of a binary vanadium(V) azide was however possible by taking advantage of the fact that the oxidation potential of an anion is lower than that of its neutral parent compound, thus avoiding the reduction of vanadium(V) to vanadium(IV) by azide. Using $[NMe_4][VF_6]$ as a starting material and reacting it with an excess of Me_3SiN_3 in acetonitrile solution resulted in the isolation of the corresponding hexaazidovanadate(V) compound [Eq. (4)].

$$[NMe_4][VF_6] + 6\,Me_3SiN_3 \xrightarrow{CH_3CN} [NMe_4][V(N_3)_6] + 6\,Me_3SiF \qquad (4)$$

$[NMe_4][V(N_3)_6]$ was isolated as a black amorphous solid that is thermally stable at room temperature but is highly shock-sensitive and explodes violently upon the slightest provocation. The intense maroon, almost black color of all the vanadium azides isolated in the course of our study is attributed to the fact that many vanadium compounds, and particularly those of vanadium(IV), are deeply colored and that this color can be enhanced by the presence of multiple azido ligands, which can act as chromophores.

The composition of $[NMe_4][V(N_3)_6]$ was established by the observed weight and its low-temperature Raman spectrum (Figure 2). The Raman spectrum of $[V(N_3)_6]^-$ is distinctively different from that of $[V(N_3)_6]^{2-}$. Not only are the antisymmetric N_3 and skeletal V–N stretching vibrations shifted to higher frequencies, as expected for an increased covalency of the azido ligands owing to the decreased formal negative charge of the anion, but also the band splittings and relative intensities differ significantly. The shift of the bands to higher frequencies with decreasing formal negative charges has previously been demonstrated for the VF_6^-, VF_6^{2-}, and VF_6^{3-} series.[29]

The predicted structures of free $[V(N_3)_6]^{2-}$ and $[V(N_3)_6]^-$ (Supporting Information, Table S17) show significant differences. In $[V(N_3)_6]^{2-}$, the VN_6 skeleton is almost perfectly

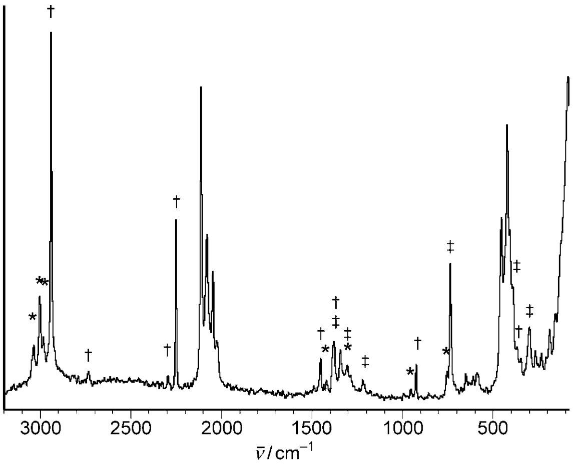

Figure 2. Low-temperature Raman spectrum of $[NMe_4][V(N_3)_6]$. Bands belonging to the NMe_4 cation are marked with an asterisk (*). Bands marked with a dagger (†) are due to a residual amount of CH_3CN solvent, and bands due to the FEP sample container are marked with a double dagger (‡).

octahedral and the azido ligands exhibit a propeller-type arrangement, resulting in approximate S_6 symmetry. In contrast, the VN_6 skeleton of $[V(N_3)_6]^-$ is significantly distorted from octahedral symmetry, with three shorter and three longer V–N bonds in *mer* positions ($\Delta(V{-}N) \approx 0.035$ Å at the B3LYP level). The structure can be visualized as being composed of two T-shaped halves, one possessing the shorter bonds and the other the longer bonds, with the crossbars of the two Ts being orthogonal to each other, forming the equatorial plane of a distorted octahedron. Furthermore, the azido ligands of $[V(N_3)_6]^-$ are more covalent than those in $[V(N_3)_6]^{2-}$, with an average N–N bond difference of 0.065 Å, and do not vary much in their ionic character. The pronounced splittings of the antisymmetric N_3 stretching modes in $[V(N_3)_6]^-$ can readily be accounted for by the increased distortion of its VN_6 skeleton and the greater variations in its V–N bond lengths, and this interpretation is further supported by the calculated vibrational spectra (Supporting Information, Table S18). The difference in the counterions, PPh_4^+ or PNP^+ versus $N(CH_3)_4^+$, the change in the anion to cation ratios, and the presence of some residual CH_3CN in the $[N(CH_3)_4][V(N_3)_6]$ sample are probably only minor contributors to these differences. The vibrational frequencies observed for the residual CH_3CN in the sample are similar to those of the free molecule in the gas phase[30] and strongly differ from those observed for bound CH_3CN in $Nb(N_3)_5(CH_3CN)$ and $Ta(N_3)_5(CH_3CN)$,[14] thus demonstrating that the acetonitrile in our $[N(CH_3)_4][V(N_3)_6]$ sample does not act as a ligand. The calculated and observed vibrational spectra and assignments of $[V(N_3)_6]^-$ are summarized in the Supporting Information, Table S18.

The fact that free $[V(N_3)_6]^-$ with d^0 vanadium(V) and no possibility for Jahn–Teller distortion is predicted to possess a much lower symmetry than $[V(N_3)_6]^{2-}$ with d^1V(+IV) and possible Jahn–Teller distortion obviously cannot be explained by the Jahn–Teller effect. The strong influence of the oxidation state of vanadium on the structure of its VX_6 anions has previously been discussed by Becker and Sawodny for the $[VF_6]^{3-}$, $[VF_6]^{2-}$ and $[VF_6]^-$ series.[29]

In summary, the first binary vanadium(IV) azides $V(N_3)_4$ and $[V(N_3)_6]^{2-}$, and vanadium(V) azide $V(N_3)_6^-$, have been prepared and characterized. At ambient temperature, the neutral tetraazide and $V(N_3)_6^-$ are very sensitive and highly explosive but the $[V(N_3)_6]^{2-}$ anion, particularly when combined with a large inert counterion, is more manageable. Furthermore, the $V(N_3)_6^-$ anion is the first binary vanadium(V) species containing a ligand other than fluorine or oxygen.

Received: November 20, 2009
Revised: June 15, 2010
Published online: August 16, 2010

Keywords: azides · electronic structure · vanadium · vibrational spectroscopy · X-ray diffraction

[1] a) Z. Dori, R. F. Ziolo, *Chem. Rev.* **1973**, *73*, 247; b) I. C. Tornieporth-Oetting, T. M. Klapötke, *Angew. Chem.* **1995**, *107*, 559; *Angew. Chem. Int. Ed. Engl.* **1995**, *34*, 511; c) T. M. Klapötke, *Chem. Ber.* **1997**, *130*, 443; d) A. Kornath, *Angew. Chem.* **2001**, *113*, 3231; *Angew. Chem. Int. Ed.* **2001**, *40*, 3135; e) W. Fraenk, T. M. Klapötke in *Inorganic Chemistry Highlights* (Eds.: G. Meyer, D. Naumann, L. Wesemann), Wiley-VCH, Weinheim, **2002**; f) J. Müller, *Coord. Chem. Rev.* **2002**, *235*, 105; g) C. Knapp, J. Passmore, *Angew. Chem.* **2004**, *116*, 4938; *Angew. Chem. Int. Ed.* **2004**, *43*, 4834.

[2] B. Neumüller, F. Schmock, K. Dehnicke, *Z. Anorg. Allg. Chem.* **1999**, *625*, 1243.

[3] A. C. Filippou, P. Portius, D. U. Neumann, K.-D. Wehrstedt, *Angew. Chem.* **2000**, *112*, 4524; *Angew. Chem. Int. Ed.* **2000**, *39*, 4333.

[4] A. C. Filippou, P. Portius, G. Schnakenburg, *J. Am. Chem. Soc.* **2002**, *124*, 12396.

[5] T. M. Klapötke, B. Krumm, P. Mayer, H. Pietrowski, O. P. Ruscitti, A. Schiller, *Inorg. Chem.* **2002**, *41*, 1184.

[6] K. Karaghiosoff, T. M. Klapötke, B. Krumm, H. Nöth, T. Schütt, M. Suter, *Inorg. Chem.* **2002**, *41*, 170.

[7] T. M. Klapötke, B. Krumm, P. Mayer, I. Schwab, *Angew. Chem.* **2003**, *115*, 6024; *Angew. Chem. Int. Ed.* **2003**, *42*, 5843.

[8] R. Haiges, J. A. Boatz, A. Vij, M. Gerken, S. Schneider, T. Schroer, K. O. Christe, *Angew. Chem.* **2003**, *115*, 6027; *Angew. Chem. Int. Ed.* **2003**, *42*, 5847.

[9] R. Haiges, A. Vij, J. A. Boatz, S. Schneider, T. Schroer, M. Gerken, K. O. Christe, *Chem. Eur. J.* **2004**, *10*, 508.

[10] R. Haiges, S. Schneider, T. Schroer, K. O. Christe, *Angew. Chem.* **2004**, *116*, 5027; *Angew. Chem. Int. Ed.* **2004**, *43*, 4919.

[11] R. Haiges, J. A. Boatz, A. Vij, V. Vij, M. Gerken, S. Schneider, T. Schroer, M. Yousufuddin, K. O. Christe, *Angew. Chem.* **2004**, *116*, 6844; *Angew. Chem. Int. Ed.* **2004**, *43*, 6676.

[12] R. Haiges, J. A. Boatz, S. Schneider, T. Schroer, M. Yousufuddin, K. O. Christe, *Angew. Chem.* **2004**, *116*, 3210; *Angew. Chem. Int. Ed.* **2004**, *43*, 3148.

[13] R. Haiges, J. A. Boatz, R. Bau, S. Schneider, T. Schroer, M. Yousufuddin, K. O. Christe, *Angew. Chem.* **2005**, *117*, 1894; *Angew. Chem. Int. Ed.* **2005**, *44*, 1860.

[14] R. Haiges, J. A. Boatz, T. Schroer, M. Yousufuddin, K. O. Christe, *Angew. Chem.* **2006**, *118*, 4948; *Angew. Chem. Int. Ed.* **2006**, *45*, 4830.

[15] R. Haiges, J. A. Boatz, M. Yousufuddin, K. O. Christe, *Angew. Chem.* **2007**, *119*, 2927; *Angew. Chem. Int. Ed.* **2007**, *46*, 2869.

[16] a) J. P. Johnson, G. K. MacLean, J. Passmore, P. S. White, *Can. J. Chem.* **1989**, *67*, 1687; b) M. J. Crawford, A. Ellern, P. Mayer, *Angew. Chem.* **2005**, *117*, 8086; *Angew. Chem. Int. Ed.* **2005**, *44*, 7874.

[17] V. Gutmann, O. Leitmann, A. Scherhaufer, H. Czuba, *Monatsh. Chem.* **1967**, *98*, 188.

[18] H.-H. Schmidtke, D. Garthoff, *Z. Naturforsch. A* **1969**, *24*, 126.

[19] K. Dehnicke, *J. Inorg. Nucl. Chem.* **1965**, *27*, 809.

[20] W. Beck, W. P. Fehlhammer, P. Pöllmann, E. Schuierer, K. Feldl, *Chem. Ber.* **1967**, *100*, 2335.

[21] W. Beck, E. Schuierer, P. Pöllmann, W. P. Fehlhammer, *Z. Naturforsch. B* **1966**, *21*, 811.

[22] J. Hanich, M. Krestel, U. Mueller, K. Dehnicke, D. Rehder, *Z. Naturforsch. B* **1984**, *39*, 1686.

[23] A. M. Golub, H. Koehler, V. V. Stopenko, *Chemistry of Pseudohalides*, Elsevier, Amsterdam, **1986**.

[24] a) Crystal data for $C_{48}H_{40}N_{18}P_2V$: $M_r = 981.86$, triclinic, space group $P\bar{1}$, $a = 10.098(3)$, $b = 10.365(3)$, $c = 12.258(4)$ Å, $\alpha = 88.498(6)$, $\beta = 75.688(6)$, $\gamma = 69.406(6)°$, $V = 1161.1(7)$ Å^3, $F(000) = 507$, ρ_{calcd} $(Z = 1) = 1.404$ g cm^{-3}, $\mu = 0.340$ mm^{-1}; approximate crystal dimensions $0.28 \times 0.20 \times 0.05$ mm^3, θ range = 1.72 to 27.59°, $Mo_{K\alpha}$ ($\lambda = 0.71073$ Å), $T = 143(2)$ K, 7186 measured data (Bruker 3-circle, SMART APEX CCD with χ-axis fixed at 54.74°, using the SMART V 5.630 program, Bruker AXS: Madison, WI, **2003**), of which 5017 ($R_{int} = 0.0241$) unique. Lorentz and polarization correction (SAINT V 6.45 program, Bruker AXS: Madison, WI, **2003**), absorption correction (SADABS program, Bruker AXS: Madison, WI, **2001**). Structure solution by the Patterson method (SHELXTL 6.14, Bruker AXS: Madison, WI, **2003**), full-matrix least-squares refinement on F^2, data to parameters ratio: 16.0:1, final R indices $[I > 2\sigma(I)]$: $R1 = 0.0666$, $wR2 = 0.1757$, R indices (all data): $R1 = 0.0955$, $wR2 = 0.1938$, GOF on $F^2 = 1.042$; b) Crystal data for $C_{72}H_{60}N_{20}P_4V$: $M_r = 1380.22$, triclinic, space group $P\bar{1}$, $a = 11.6921(10)$, $b = 12.6510(10)$, $c = 24.433(2)$ Å, $\alpha = 93.9940(10)$, $\beta = 101.4690(10)$, $\gamma = 103.0870(10)°$, $V = 3424.9(5)$ Å^3, $F(000) = 1430$, ρ_{calcd} $(Z = 2) = 1.338$ g cm^{-3}, $\mu = 0.298$ mm^{-1}; approximate crystal dimensions $0.24 \times 0.19 \times 0.18$ mm^3, θ range = 1.66 to 27.50°, $Mo_{K\alpha}$ ($\lambda = 0.71073$ Å), $T = 193(2)$ K, 21385 measured data (Bruker 3-circle, SMART APEX CCD with χ-axis fixed at 54.74°, using the SMART V 5.630 program, Bruker AXS: Madison, WI, **2003**), of which 14837 ($R_{int} = 0.0292$) unique. Lorentz and polarization correction (SAINT V 6.45 program, Bruker AXS: Madison, WI, **2003**), absorption correction (SADABS program, Bruker AXS: Madison, WI, **2001**). Structure solution by the Patterson method (SHELXTL 6.14, Bruker AXS: Madison, WI, **2003**), full-matrix least-squares refinement on F^2, data to parameters ratio: 17.0:1, final R indices $[I > 2\sigma(I)]$: $R1 = 0.0616$, $wR2 = 0.1276$, R indices (all data): $R1 = 0.1096$, $wR2 = 0.1537$, GOF on $F^2 = 1.011$. CCDC 288159 ($C_{48}H_{40}N_{18}P_2V$) and CCDC 768813 ($C_{72}H_{60}N_{20}P_4V$) contain the supplementary crystallographic data for this paper. These data can be obtained free of charge from The Cambridge Crystallographic Data Centre via www.ccdc.cam.ac.uk/data_request/cif.

[25] T. M. Klapötke, H. Nöth, T. Schütt, M. Warchhold, *Angew. Chem.* **2000**, *112*, 2197; *Angew. Chem. Int. Ed.* **2000**, *39*, 2108.

[26] T. M. Klapötke, B. Krumm, M. Scherr, R. Haiges, K. O. Christe, *Angew. Chem.* **2007**, *119*, 8840; *Angew. Chem. Int. Ed.* **2007**, *46*, 8686.

[27] J. Honzicek, M. Erben, I. Cisarova, J. Vinklarek, *Appl. Organomet. Chem.* **2005**, *19*, 102.

[28] M. Herberhold, A.-M. Dietel, W. Milius, *Z. Anorg. Allg. Chem.* **1999**, *625*, 1885.

[29] R. Becker, W. Sawodny, *Z. Naturforsch. B* **1973**, *28*, 360.

[30] T. Shimanouchi, *Natl. Stand. Ref. Data Ser. (U. S. Natl. Bur. Stand.)* **1972**, 39, 84.

[31] K. O. Christe, W. W. Wilson, C. J. Schack, R. D. Wilson, *Inorg. Synth.* **1986**, *24*, 39.

[32] R. Haiges, T. Schroer, M. Yousufuddin, K. O. Christe, *Z. Anorg. Allg. Chem.* **2005**, *631*, 2691.

[33] K. Licht, P. Koehler, H. Kriegsmann, *Z. Anorg. Allg. Chem.* **1975**, *415*, 31.

[34] H. Bürger, *Spectrochim. Acta Part A* **1968**, *24*, 2015.

[35] a) C. Møller, M. S. Plesset, *Phys. Rev.* **1934**, *46*, 618; J. A. Pople, J. S. Binkley, R. Seeger, *Int. J. Quantum Chem.* **1976**, *S10*, 1; b) M. J. Frisch, M. Head-Gordon, J. A. Pople, *Chem. Phys. Lett.* **1990**, *166*, 275; c) J. Bartlett, D. M. Silver, *Int. J. Quantum Chem. Symp.* **1975**, *9*, 1927.

[36] a) A. D. Becke, *J. Chem. Phys.* **1993**, *98*, 5648; b) P. J. Stephens, F. J. Devlin, C. F. Chablowski, M. J. Frisch, *J. Phys. Chem.* **1994**, *98*, 11623; c) R. H. Hertwig, W. Koch, *Chem. Phys. Lett.* **1997**, *268*, 345; d) S. H. Vosko, L. Wilk, M. Nusair, *Can. J. Phys.* **1980**, *58*, 1200.

[37] a) Y. Sakai, E. Miyoshi, M. Klobukowski, S. Huzinaga, *J. Chem. Phys.* **1997**, *106*, 8084; b) T. Noro, M. Sekiya, T. Koga, *Theor. Chem. Acc.* **1997**, *98*, 25; c) Y. Osanai, M. S. Mon, T. Noro, H. Mori, H. Nakashima, M. Klobukowski, E. Miyoshi, *Chem. Phys. Lett.* **2008**, *452*, 210; d) T. Noro, M. Sekiya, T. Koga, H. Matsuyama, *Theor. Chem. Acc.* **2000**, *104*, 146.

[38] a) M. W. Schmidt, K. K. Baldridge, J. A. Boatz, S. T. Elbert, M. S. Gordon, J. H. Jensen, S. Koseki, N. Matsunaga, K. A. Nguyen, S. Su, T. L. Windus, M. Dupuis, J. A. Montgomery, *J. Comput. Chem.* **1993**, *14*, 1347; b) M. S. Gordon, M. W. Schmidt in *Theory and Applications of Computational Chemistry: The First Forty Years* (Eds.: C. E. Dykstra, G. Frenking, K. S. Kim, G. E. Scuseria), Elsevier, Amsterdam, **2005**, pp. 1167–1189.